

# Tunable dispersion compensation by a rotating cylindrical lens

Michael E. Durst,\* Demirhan Kobat, and Chris Xu

School of Applied and Engineering Physics, Cornell University, Ithaca, New York 14853, USA

\*Corresponding author: med43@cornell.edu

Received January 26, 2009; revised March 2, 2009; accepted March 4, 2009;  
posted March 13, 2009 (Doc. ID 106754); published April 7, 2009

We present a technique for tunable dispersion compensation that is low cost, high speed, and has a large tuning range. By rotating a cylindrical lens at the Fourier plane of a folded  $4f$  grating pair system, the group-velocity dispersion can be tuned over a range greater than  $10^5$  fs<sup>2</sup>, sufficient for compensating the dispersion of several meters of optical fiber. © 2009 Optical Society of America

OCIS codes: 230.2035, 320.5520, 190.4180.

Various applications in ultrafast and nonlinear optics require a tunable dispersion compensator. For example, because the fluorescence signal in multiphoton microscopy (MPM) depends inversely on the pulse width, one can maximize the signal by compensating the dispersion along the optical path [1]. Dispersion compensation in MPM is particularly important when highly dispersive elements such as acousto-optic or electro-optic modulators are used [2]. Another application is for simultaneous spatial and temporal focusing (SSTF), where a temporal focus can be scanned axially by tuning the dispersion [3]. Typical methods for compensating dispersion include prism pairs [4] and grating pairs [5], but their tuning speed is limited by the mechanical translation of these bulky optical elements. Other techniques have been developed to simplify these setups by using a single diffractive element in a folded system [6], but ultimately the tuning of a  $4f$  grating setup is still accomplished by translating the components over large distances [7].

Several electronically or thermally tuned devices exist. For fiber applications, thermally tuned fiber Bragg gratings [8], electronically driven phase modulators [9], and waveguide grating routers combined with deformable mirrors or phase modulators [10] can all tune the dispersion at high speed, but these devices cannot support ultrashort pulse propagation. Free-space electronically addressed devices, such as acousto-optic modulators (AOMs) [11], spatial light modulators (SLMs) [12], and deformable mirrors [13], can achieve programmable and high-speed dispersion tuning. In these devices, a pixelated array can impose a spectral phase with arbitrary shape but at a high cost and with limited tuning range. The advantage of these devices is the capability to compensate for higher-order dispersion, but this is unnecessary for many practical applications. For example, when 50 fs or longer duration pulses are used in MPM [14] and SSTF for remote axial scanning [3], compensation of the second-order group-delay dispersion (GDD) is sufficient.

We describe here a technique for tunable dispersion compensation by using a rotating cylindrical lens. We use a grating, a spherical collimating lens, and a mirror in a folded  $4f$  system. Our setup is simi-

lar to those used with deformable mirrors and reflective SLMs except we place a plano-convex cylindrical lens at the Fourier plane (Fig. 1). The optical path length variation across the spectral components due to the curvature of the lens imposes a quadratic phase across the spectrum. Rotating the cylindrical lens changes the effective radius of curvature, thus changing the amount of GDD in the system. By using a cylindrical lens of a sufficiently long focal length, a large dispersion tuning range can be achieved while introducing negligible spatial distortion due to the focusing effect of the cylindrical lens. Because the cylindrical lens is rotated rather than linearly translated, the output beam exhibits directional stability, and the motion can be made high speed with a simple motor. Thus, high-speed tunable dispersion compensation is realized by rotating a cylindrical lens in a  $4f$  grating pair setup. Our technique is low cost, high speed, and has a large range that is sufficient for compensating the dispersion of several meters of optical fiber.

A glass plano-convex lens is shown at the Fourier plane of a folded  $4f$  grating pair setup in Fig. 1. We derive an expression for the optical path length due to the curvature of the lens as a function of the transverse position  $x$ :

$$z = nd + (n - 1)[\sqrt{R^2 - x^2} - R], \quad (1)$$

where  $z$  is the path length,  $n$  is the refractive index of the glass,  $d$  is the thickness of the lens at its center,  $R$  is the radius of curvature of the lens, and  $x$  is the distance from the center of the lens. Dropping the constant phase term and assuming that the focal length

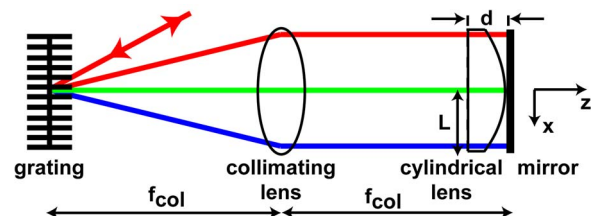


Fig. 1. (Color online) GDD compensation device: folded  $4f$  grating pair setup with a cylindrical lens at the Fourier plane.

of the lens is large ( $R \gg x$ ), Eq. (1) can be approximated as  $z \approx -x^2/(2f_{\text{cyl}})$ , where  $f_{\text{cyl}}$  is the focal length of the cylindrical lens. With a simple coordinate rotation that takes into account the quadratic spatial profile of the lens, the effective focal length becomes  $f_{\text{eff}} = f_{\text{cyl}}/\cos^2 \theta$  as the cylindrical lens is rotated about the optical axis by an angle  $\theta$ . Taking into account the double-pass configuration, the phase delay due to the thickness of the lens can be related to the GDD by

$$-\frac{kx^2}{f_{\text{eff}}} = \frac{1}{2} \text{GDD} \left( x \frac{\Omega}{2L} \right)^2, \quad (2)$$

where  $k$  is the wavevector corresponding to the center wavelength ( $\lambda$ ) and  $L$  is the half-width of the lens.  $\Omega$  is the total optical bandwidth across the cylindrical lens, which is determined by the incident angle, the groove density of the grating, and the focal length of the collimating lens ( $f_{\text{col}}$ ). We note that  $\Omega$  is independent of the pulse bandwidth. Solving for the GDD,

$$\text{GDD} = -\frac{2k}{f_{\text{eff}}} \left( \frac{2L}{\Omega} \right)^2 = -\frac{4\pi}{\lambda f_{\text{cyl}}} \left( \frac{2L}{\Omega} \cos \theta \right)^2. \quad (3)$$

As shown in Eq. (3), the amount of GDD imparted on the beam can be tuned by rotating the cylindrical lens. For  $f_{\text{cyl}} = 10$  m,  $L = 2.54$  cm,  $\lambda = 775$  nm, and  $\Omega = 1.79 \times 10^{14}$  Hz ( $f_{\text{col}} = 30$  cm, a grating with a groove density of 1800 lines per mm, and a  $39^\circ$  incident angle on the grating), the maximum GDD will be  $-1.3 \times 10^5$  fs<sup>2</sup>.

The experimental setup to characterize the GDD compensation device is shown in Fig. 1. We use a mode-locked Ti:sapphire laser (Spectra-Physics) centered at 775 nm with approximately 10 nm (FWHM) of bandwidth. A ruled diffraction grating with a groove density of 1800 lines per mm separates the beam into its monochromatic components, which are then collimated by a spherical lens ( $f_{\text{col}} = 30$  cm). At the Fourier plane, we place a folding mirror and a plano-convex cylindrical lens ( $f_{\text{cyl}} = 10$  m, CVI Melles Griot SCX-50.8-5000.0-C) on a rotation stage. We measure the pulse width of the beam exiting the GDD compensation device using an interferometric second-order autocorrelator, which has a GaAsP photodiode as the nonlinear element. The pulse width for different rotation angles of the cylindrical lens are shown in Fig. 2. We were able to broaden the pulse from 80 fs with no curvature ( $\theta = 90^\circ$ ) to 3.3 ps with full curvature [ $\theta = 0^\circ$ , see autocorrelation trace in

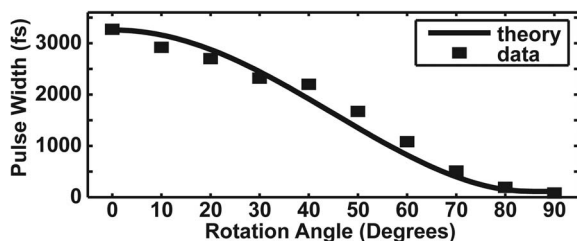


Fig. 2. Pulse width versus rotation angle of the cylindrical lens. Squares, autocorrelation data; solid curve, theoretical curve based on Eq. (3).

Fig. 3(a)], corresponding to an induced GDD of  $-1.26 \times 10^5$  fs<sup>2</sup> (sech shape). Note that the pulse width follows a cosine-squared dependence on rotation angle (solid curve in Fig. 2). The experimentally obtained GDD tuning range and the dependence on the rotation angle  $\theta$  agree well with the theoretical predictions of Eq. (3). To demonstrate the utility of the device for fiber delivery, we couple the beam into 2 m of standard single-mode fiber (SSMF), which has an estimated dispersion value of  $7.6 \times 10^4$  fs<sup>2</sup> at this wavelength. The coupled power into the SSMF was kept sufficiently low to avoid any fiber nonlinearity. By rotating the cylindrical lens, we are able to recover an 80 fs pulse out of the fiber [see autocorrelation trace in Fig. 3(b)].

To determine the spatial and temporal quality of the pulses, we measure the dependence of the two-photon-induced photocurrent by focusing the beam onto a GaAsP photodiode through  $90^\circ$  rotation of the cylindrical lens [Fig. 4(a)]. The two-photon-induced current closely follows the expected inverse pulse-width dependence, as shown by the solid curve in Fig. 4(a). It is well known that the amount of two-photon excitation depends sensitively on the spatial and temporal quality of the excitation beam. Results in Fig. 4(a) indicate that the spatial and temporal quality of the pulse is not degraded after the dispersion compensation device. To demonstrate the superb beam-pointing stability of this setup while tuning the GDD, we couple the output beam into an SSMF and measure the output power as a function of rotation angle  $\theta$  without changing the fiber coupling setup [Fig. 4(b)]. The output power varies by approximately 2.5% throughout the GDD tuning range. We also measure the point-spread function (PSF) of the output beam by imaging 200 nm fluorescent beads in a two-photon laser scanning microscope. Using a 0.57 NA objective lens, the lateral FWHM of the bead image is  $0.5 \mu\text{m}$  and the axial FWHM is  $3.6 \mu\text{m}$ , which is in agreement with theory [1]. Because a rotation angle of  $0^\circ$  dramatically broadens the pulse, a 40 cm SF11 glass rod is added to the beam path to partially negate the pulse broadening and increase the signal at  $\theta = 0^\circ$ . The PSF does not change size or shape as we rotate the cylindrical lens from  $0^\circ$  to  $90^\circ$  (Fig. 4(a) insets), thus demonstrating the suitability of our device for imaging applications.

Spatial-temporal coupling is a concern in such a 4f setup, similar to dispersion tuning devices using deformable mirrors or SLMs [12,13]. Our measure-

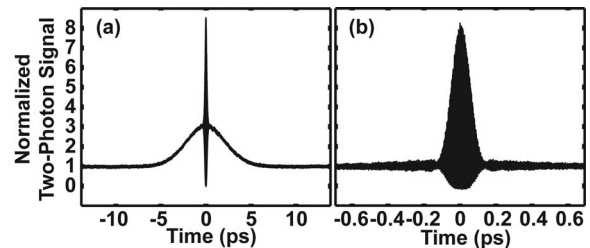


Fig. 3. Interferometric second-order autocorrelations of the pulse exiting the dispersion compensation device (a) with maximum curvature ( $\theta = 0^\circ$ ) and (b) with 2 m of SSMF at  $\theta = 30^\circ$ .

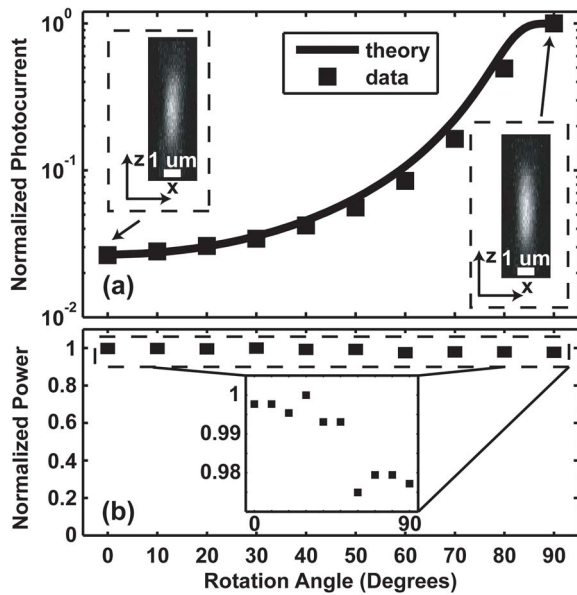


Fig. 4. (a) Normalized two-photon induced current (log scale) as a function of the rotation angle of the cylindrical lens. Insets, normalized PSF of output beam at  $\theta=0^\circ$  and  $\theta=90^\circ$ . (b) Normalized power coupled into an SSMF as a function of cylindrical lens angle. Inset, enlarged view of the power variation.

ments show that the bandwidth coupled into a SSMF varied by approximately 20% over the entire GDD tuning range when the input pulse bandwidth is increased to 17 nm (FWHM), indicating non-negligible spatial chirp due to the curvature of the cylindrical lens. For our experimental bandwidth of 10 nm, the bandwidth coupled into SSMF varies within 1 nm throughout the tuning range. While such spatial-temporal coupling can be reduced by using a longer focal length cylindrical lens, the GDD tuning range will be proportionally reduced [Eq. (3)]. Thus there is a compromise between the maximum GDD tuning range and the shortest pulse duration. As shown by the experimental results, we were able to obtain  $1.26 \times 10^5 \text{ fs}^2$  GDD tuning with an 80 fs pulse in this particular setup.

It is informative to compare the performance of our GDD compensator with existing tunable GDD products that employ AOMs and prism pair configurations. Folded prism-pair designs are low cost but are limited in range by the size of the prism and in speed by the mass of the folding mirror. With AOMs as the dispersive elements, the GDD can be tuned at high

speed, but the available tuning range is similar to the prism-pair design with one order of magnitude greater cost. Our components are low cost, available off the shelf, and yield a broad tuning range of greater than  $10^5 \text{ fs}^2$ . We further note that the sign of the dispersion in our device can be changed by switching from a convex lens to a concave lens. A fixed offset of the tuning range can also be obtained by adding an extra fixed lens at the Fourier plane. Furthermore, an all-reflecting geometry can be accomplished with a spherical collimating mirror and a rotating cylindrical mirror.

In this Letter, we have demonstrated a technique for tunable dispersion compensation by rotating a cylindrical lens at the Fourier plane of a folded  $4f$  grating pair system. The GDD can be tuned over a range greater than  $10^5 \text{ fs}^2$ , sufficient for compensating the dispersion of several meters of SSMF. This tunable GDD compensator is low cost, capable of high speeds, and has a large tuning range.

This research was made possible by the National Institutes of Health (NIH) (grant R21CA129648).

## References

1. W. R. Zipfel, R. M. Williams, and W. W. Webb, *Nat. Biotechnol.* **21**, 1368 (2003).
2. V. Iyer, B. E. Losavio, and P. Saggau, *J. Biomed. Opt.* **8**, 471 (2003).
3. M. E. Durst, G. Zhu, and C. Xu, *Opt. Commun.* **281**, 1805 (2008).
4. R. L. Fork, O. E. Martinez, and J. P. Gordon, *Opt. Lett.* **9**, 150 (1984).
5. O. E. Martinez, *IEEE J. Quantum Electron.* **23**, 59 (1987).
6. S. Akturk, X. Gu, M. Kimmel, and R. Trebino, *Opt. Express* **14**, 10108 (2006).
7. Y. Chen and X. Li, *Opt. Express* **12**, 5978 (2004).
8. N. Q. Ngo, S. Y. Li, R. T. Zheng, S. C. Tjin, and P. Shum, *J. Lightwave Technol.* **21**, 1575 (2003).
9. J. van Howe and C. Xu, *J. Lightwave Technol.* **24**, 2662 (2006).
10. D. M. Marom, C. R. Doerr, M. A. Cappuzzo, C. Evans Yifan, A. Wong-Foy, L. T. Gomez, and S. Chandrasekhar, *J. Lightwave Technol.* **24**, 241 (2006).
11. P. Tournois, *Opt. Commun.* **140**, 245 (1997).
12. A. M. Weiner, D. E. Leaird, J. S. Patel, and J. R. Wullert, *Opt. Lett.* **15**, 326 (1990).
13. E. Zeek, K. Maginnis, S. Backus, U. Russek, M. Murnane, G. Mourou, H. Kapteyn, and G. Vdovin, *Opt. Lett.* **24**, 493 (1999).
14. J. B. Guild, C. Xu, and W. W. Webb, *Appl. Opt.* **36**, 401 (1997).